Materials Chemistry and Physics 130 (2011) 126–133

Contents lists available at ScienceDirect

Materials Chemistry and Physics

journal homepage: www.elsevier.com/locate/matchemphys

Mechanical and electrical properties of novel poly(ether ether ketone)/carbon nanotube/inorganic fullerene-like WS_2 hybrid nanocomposites: Experimental measurements and theoretical predictions

Ana M. Díez-Pascual, Mohammed Naffakh*, Marián A. Gómez-Fatou

Department of Physics and Engineering, Institute of Polymer Science and Technology, CSIC, Juan de la Cierva 3, 28006 Madrid, Spain

ARTICLE INFO

Article history:
Received 23 March 2011
Received in revised form 12 May 2011
Accepted 12 June 2011

Keywords:
Composite materials
Mechanical properties
Fracture and toughness
Electrical conductivity

ABSTRACT

The mechanical and electrical properties of poly(ether ether ketone) (PEEK) based hybrid nanocomposites incorporating single-walled carbon nanotubes (SWCNTs) and inorganic fullerene-like tungsten disulfide (IF-WS_2) nanoparticles have been extensively investigated from both experimental and theoretical point of views. Dynamic mechanical studies revealed a remarkable increase in the storage modulus and glass transition temperature of the matrix by the inclusion of both nanofillers. Moreover, tensile and flexural tests indicated significant enhancements in stiffness and strength, attributed to synergistic reinforcement effects combined with strong PEEK–SWCNT interfacial interactions. The Young's modulus of these nanocomposites was fairly well predicted by simple theoretical models such as the rule of mixtures. The hybrids with SWCNT content equal or higher than 0.5 wt% exhibited semiconducting behaviour and the temperature dependence of their electrical conductivity followed a fluctuation-induced tunnelling model. Enhanced overall performance was found for composites prepared by a single-step melt-blending process compared to those manufactured in two stages. The addition of both nanoreinforcements opens up new opportunities for the development of high-performance multifunctional materials suitable for industrial applications.

1. Introduction

Over the last decades, carbon nanotubes (CNTs) have attracted a lot of interest because of their outstanding thermal, electrical and mechanical properties, attributed to their high aspect ratio and nanoscale dimensions [1]. These excellent properties make them useful for fabricating nanodevices and developing multifunctional composite materials [2]. However, due to their rigidity, chemical inertness and strong π–π interactions, pure CNTs cannot be processed, since they are difficult to dissolve or disperse in common organic solvents or polymer matrices. To address this problem, several methods have been developed, i.e. surfactant assisted dispersion [3], high power sonication [4], polymer wrapping [5], and surface modification such as inorganic coating [6]. In this regard, new hybrid nanocomposite materials with synergetic behaviours due to interactions between organic and inorganic components have been fabricated [7,8]; they exhibit a large number of potential applications, mainly in electronic nanodevices, gas sensing and catalysis. Particularly interesting are nanocomposites involving nanoparticles of metal oxide or layered transition metal chalcogenide (MoS_2, WS_2, NbS_2), which spontaneously form closed-cage structures similar to carbon fullerenes. These non-carbon materials were discovered by Tenne in 1992 [9], and are named as inorganic fullerene-like (IF). The IF nanoparticles exhibit superior properties such as high modulus and low friction coefficient [10], attributed to their small spherical size, closed structure and chemical inertness. They have been used as favourable solid lubricants under severe conditions. Recently, several studies have been reported on the incorporation of these inorganic fillers into various matrices [11–13], including epoxy, polypropylene, and poly(phenylene sulphide), to improve the thermal, mechanical and tribological properties of the nanocomposites.

Poly(ether ether ketone) (PEEK) is a semicrystalline thermoplastic polymer with excellent mechanical properties [14,15] such as high strength, modulus and toughness, which combined with its excellent thermal stability and chemical inertness make it suitable for a wide range of commercial and industrial applications, from medicine to the automobile and aerospace industries. To extend its structural applications, it is of great relevance to improve the mechanical performance of PEEK by reinforcing it with nanofillers. Studies by Shaffer et al. [16,17] revealed a linear increase in the tensile strength and stiffness of PEEK/vapour grown carbon nanofibres (CNF) with increasing CNF content up to 15 wt%. In recent works, we also demonstrated a significant

* Corresponding author. Tel.: +34 915622900; fax: +34 915644853.
E-mail address: mnaffakh@ictp.csic.es (M. Naffakh).

0254-0584/$ – see front matter © 2011 Elsevier B.V. All rights reserved.
doi:10.1016/j.matchemphys.2011.06.019

improvement in the mechanical properties of PEEK by the incorporation of small amounts of single-walled carbon nanotubes (SWCNTs) [18,19] or IF-WS_2 nanoparticles [20]. The inclusion of much cheaper (in comparison with CNF or SWCNT) inorganic particles into PEEK is of basic interest for the purposes of processability and mechanical enhancement at low reinforcement content. PEEK/IF-WS_2 nanocomposites exhibit higher thermal conductivity, tensile modulus and strength than the pure polymer [20]. However, the addition of these nanofillers does not improve the electrical behaviour of the matrix.

In a preceding paper [21], we described the preparation and thermal characterization of PEEK/SWCNT/IF-WS_2 hybrid composites that combine the advantages of both types of nanofillers. They were manufactured by melt-blending, a simple processing technique easy to scale up. The developed nanocomposites display significantly higher thermal stability than the pure matrix, which is of great interest for potential high-temperature applications. The principal aim of the current work is to extensively investigate their mechanical properties, comparing the results with the predictions of different theoretical models. Moreover, their electrical conductivity as a function of temperature has been also analyzed. Interestingly, the properties of these hybrids can be easily tuned by modifying the SWCNT/IF-WS_2 contents.

2. Experimental

2.1. Materials

Poly(ether ether ketone) (PEEK) 150P ($M_w \sim 40{,}000\ g\ mol^{-1}$, $d_{25\,^\circ C} = 1.32\ g\ cm^{-3}$) was supplied by Victrex (UK). The polymer was ball-milled in order to reduce its particle size and kept in a dry environment before blending. CVD acid purified SWCNTs ($d_{25\,^\circ C} = 2.1\ g\ cm^{-3}$, diameter: 1–2 nm, length: 0.5–2 μm, purity > 90%, COOH groups ~2.7%) were purchased from Cheap Tubes Inc. (VT, USA). Inorganic fullerene-like tungsten disulfide (IF-WS_2) nanoparticles (NanoLub™, $d_{25\,^\circ C} = 7.50\ g\ cm^{-3}$, average diameter = 80 nm, aspect ratio ~1.4) were provided by Nanomaterials (Israel).

2.2. Nanocomposite preparation

The hybrid nanocomposites were prepared by melt-blending following two different procedures. In the first approach, different weight fractions of SWCNTs (x) and IF-WS_2 (y) (x/y = 0.9/0.1, 0.5/0.5, and 0.1/0.9 wt%) were simultaneously mixed with the PEEK powder (~40 g). Each mixture was dispersed in 200 mL of ethanol and homogenized by mechanical stirring and bath ultrasonication for 30 min. The resulting dispersions were dried under vacuum at 50 °C until the solvent was completely evaporated. Subsequently, the melt-compounding of the solid dispersions was performed using a Haake Rheocord 90 extruder operating at 380 °C, with a rotor speed of 150 rpm and mixing time of 20 min. The second procedure was carried out by incorporating the nanofillers in two stages. Firstly, the SWCNTs (x = 0.5 and 0.9 wt%) were mixed with the polymer powder and subjected to the indicated treatments in ethanol media. Then, the dispersions were extruded at 380 °C for 10 min. Secondly, the corresponding amount of IF-WS_2 (y = 0.5 and 0.1 wt%, respectively) was added into the extruder and mixed with the PEEK/SWCNT melt for another 10 min. The samples were cooled to room temperature and finally pressed into thin films to be used for the different characterizations. For comparative purposes, reference composites incorporating 1.0 wt% SWCNTs (x = 1) or IF-WS_2 (y = 1) were also manufactured in the same way. To simplify the nomenclature throughout the text, nanocomposites prepared in two steps are designated by (*).

2.3. Scanning electron microscopy

The surface of impact fractured specimens was observed using a Philips XL 30 ESEM microscope, operating at 25 kV and an intensity of 9×10^{-9} A. To avoid charge accumulation during electron irradiation, samples were covered with a ~5 nm overlayer of an Au–Pd (80–20) alloy in a Balzers SDC 004 evaporator, using a covering time of 242 s at 20 mA.

2.4. Dynamic mechanical analysis

The dynamic mechanical performance of the nanocomposites was analyzed using a Mettler DMA 861 dynamic mechanical analyzer. The instrument operated in the tensile mode, using rectangular shaped samples of ~19.5 mm × 4 mm × 0.5 mm. Prior to the measurements, a dynamic strain sweep experiment was carried out for each type of composite to identify the linear amplitude strain viscoeleastic region. DMA tests were performed in the temperature range between −130 and 260 °C, at a heating rate of 2 °C min^{-1} and frequencies of 0.1, 1 and 10 Hz. A dynamic force of 6 N oscillating at fixed frequency and amplitude of 30 μm was used.

2.5. Tensile and flexural tests

Tensile and flexural properties of the composites were measured with an INSTRON 4204 tester at room temperature and 50 ± 5% relative humidity, using a crosshead speed of 1 mm min^{-1} and a load cell of 1 kN. Tensile dog-bone specimens (Type V) and rectangular flexural bars (length = 40 mm, width = 5 mm and thickness = 2 mm) were employed, as specified in the UNE-EN ISO 527-1 and 178 standards, respectively. All the samples were conditioned for 24 h before the measurements. 5 specimens for each type of composite were tested to ensure reproducibility.

2.6. Charpy impact tests

Charpy notched impact strength measurements were carried out at room temperature using a CEAST Fractovis dart impact tester. A hammer mass of 1.096 kg impacted at a constant velocity of 3.60 m s^{-1} (giving a total kinetic energy at impact of 7.10 J) on notched specimen bars (length = 33 mm, width = 10 mm and thickness = 3 mm), with a V-shape notch of tip radius = 0.25 mm and depth = 2 mm, as described in the UNE-EN ISO 179 standard. The reported data correspond to the average value of 6 specimens.

2.7. Electrical conductivity

Electrical conductivity measurements as a function of temperature were performed using a source meter (Keithley 2635A) and a 2182A nanovoltmeter to measure current bias and voltage reading. The sample was placed in a temperature controlled chamber, and the temperature was checked with a sensor equipped with a platinum thermocouple. Silver conductive epoxy paint electrodes were applied on both sample surfaces to guarantee well-aligned electrodes of exactly the same size. A maximum voltage of 20 V was applied to avoid melting or degradation of the polymer due to Joule heating; the voltage was cycled 5 times in the range 0–20 V. The resistance (R) was obtained as the slope of the voltage–current plot. The conductivity (σ) was calculated according to the expression: $\sigma = t/R \times A$, where A and t are the area and thickness of the sample, respectively. At least 3 specimens of each type of composite were tested to get an average value.

3. Results and discussion

3.1. Dynamic mechanical properties

The dynamic mechanical behaviour of the hybrid composites has been investigated in order to ascertain changes in their stiffness as a function of temperature. DMA tests over a wide range of temperature are sensitive to the transitions and relaxation processes of the resin in the composite, and provide information about the filler–matrix interfacial interactions. Fig. 1a shows the temperature dependence of the storage modulus (E') for PEEK and nanocomposites with different SWCNT/IF-WS_2 weight fractions at a frequency of 1 Hz. Their E' values at 25, 100 and 200 °C are collected in Table 1. The storage modulus is indicative of the elastic energy stored in the composite, and is highly affected by its composition, state of dispersion of the fillers and their interfacial adhesion with the matrix. At temperatures below the glass transition, samples reinforced with 1.0 wt% SWCNTs or IF-WS_2 exhibit ~21 and 34% higher E' than PEEK, respectively. Regarding the different hybrids, significantly larger E' enhancements are found for those prepared by concurrent dispersion of both nanofillers. At 25 °C, the inclusion of x/y = 0.1/0.9, 0.5/0.5 and 0.9/0.1 raises the matrix modulus by an average of 39, 47 and 31%, respectively, whilst for composites fabricated in two stages with x/y = 0.5/0.5 and 0.9/0.1 the increments are only of 29 and 23%; qualitatively similar trends can be observed at 200 °C. Interestingly, for both preparation procedures, samples containing the same amount of both fillers present the highest E', which should be ascribed to synergistic reinforcement effects. This is in agreement with the observations from the ATR-FTIR spectra of the nanocomposites (see Supplementary Information, Fig. 1S) which evidenced the existence of SWCNT–matrix interactions, particularly stronger for the sample with x/y = 0.5/0.5. The discrepancies between composites that followed different manufacturing

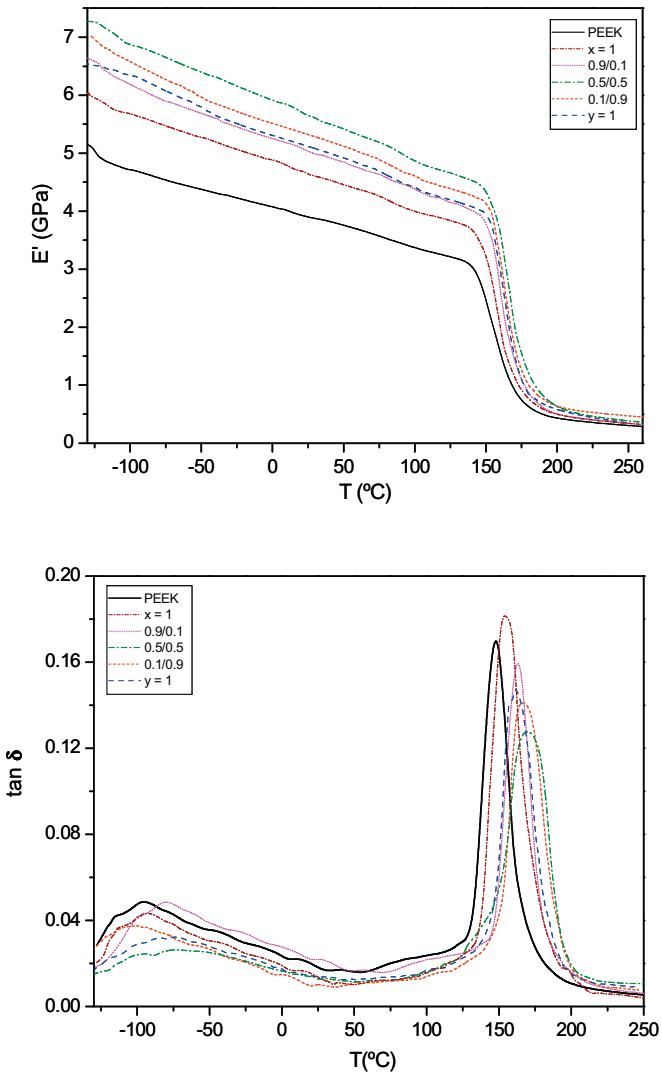

Fig. 1. Evolution of the storage modulus E' (a) and tan δ (b) as a function of temperature, at a frequency of 1 Hz, for PEEK and the hybrid nanocomposites incorporating different concentrations of SWCNTs and IF-WS_2. For comparison, data of composites including a single type of filler are also included in the plot.

approaches could be related to defects generated on the nanotube walls during melt-blending, since in a single-step process the CNTs could be more easily exfoliated under shear. Moreover, the longer the mixing time of the IF-WS_2 nanoparticles, the lower the viscosity of the matrix is; this facilitates the dispersion of the SWCNTs, thereby leading to improved properties. According to SEM observations [21], SWCNTs simultaneously mixed with the IF-WS_2 are more homogeneously distributed through the matrix, leading to larger nanotube-matrix effective contact area, which is reflected in higher E'. Furthermore, homogenously dispersed SWCNTs have higher aspect ratio than nanotube agglomerates, making them more effective for composite reinforcement.

On the other hand, our experimental data reveal a substantial drop in the storage modulus of all the composites between 150 and 200 °C, interval which corresponds to the glass transition. At higher temperatures, smaller differences are found between E' of samples prepared by the two different procedures. In general, the relative increment in modulus in comparison with PEEK rises with increasing temperature. Thus, at 200 °C, the nanocomposite with $x/y = 0.1/0.9$ exhibits about 60% E' enhancement. This indicates that the stiffening effect is more pronounced above the softening point of the matrix, which could be explained considering that the modulus of the SWCNTs changes only slightly with temperature [22]. These results are consistent with DMA studies on PEEK/CNF composites prepared by injection moulding [17], which showed higher relative increase in the matrix stiffness above than below the T_g.

Fig. 1b displays the evolution of tan δ (ratio of the loss to storage modulus) as a function of temperature; two maximums can be observed: a low broad peak at lower temperatures (β relaxation), ascribed to motions of the ketone groups, and an intense peak (α relaxation) related to the T_g. The addition of nanofillers leads to a decrease in tan δ over the studied temperature range. Furthermore, the relaxation peaks become wider and shift to higher temperatures, indicating that these nanofillers restrict the mobility of the PEEK chains. For binary composites with $x = 1$ or $y = 1$, T_g increases by 5 and 14 °C, respectively (Table 1). With respect to the different hybrids, the temperature increment is remarkably higher for those prepared in a single-stage process. In these composites, the addition of $x/y = 0.1/0.9$, 0.5/0.5 and 0.9/0.1 raises the T_g of the matrix by about 18, 22 and 13 °C, respectively, whereas those fabricated in two stages incorporating $x/y = 0.9/0.1$ and 0.5/0.5 only show increases of 7 and 11 °C. The noticeable T_g enhancement in the former systems should be ascribed to the strong obstacle on polymer chain diffusion imposed by the presence of both nanofillers homogenously dispersed through the matrix. It is worthy to note that the improvements in E' and T_g obtained in the samples prepared by simultaneous dispersion of 0.5 wt% contents of SWCNTs and IF-WS_2 are higher than those attained in PEEK nanocomposites reinforced with 1.0 wt% SWCNTs wrapped in polyetherimide [19] or polysulfone [23]. This suggests that the addition of these nanoparticles is a more effective approach to improve the SWCNT dispersion than the wrapping in compatibilizing agents.

The maximum values of tan δ (tan δ_{max}) for the different studied nanocomposites are collected in Table 1; it is found that the inclusion of 1.0 wt% SWCNTs leads to a slight increase (~7%) in the height of tan δ peak, whilst the incorporation of the same amount of

Table 1
Storage modulus E' at 25, 100 and 200 °C, glass transition temperature T_g, tan δ maximum value and width at half maximum β for the different PEEK composites, obtained from DMA measurements at a frequency of 1 Hz.

SWCNT (wt%)	WS_2 (wt%)	$E'_{25\,°C}$ (GPa)	$E'_{100\,°C}$ (GPa)	$E'_{200\,°C}$ (GPa)	T_g (°C)	Tan δ_{max} (a.u.)	β (°C)
0	0	3.83	3.32	0.43	147.8	0.168	19.0
1	0	4.63	3.97	0.51	153.9	0.179	25.4
0	1	5.12	4.36	0.59	163.3	0.147	21.8
0.1	0.9	5.32	4.59	0.68	166.4	0.141	27.9
0.5	0.5	5.65	4.86	0.62	170.2	0.126	30.1
0.9	0.1	5.02	4.41	0.53	160.9	0.161	23.6
0.5[a]	0.5[a]	4.93	4.27	0.46	159.2	0.160	22.2
0.9[a]	0.1[a]	4.71	4.18	0.63	155.0	0.163	18.5

[a] Nanocomposites obtained by a two-step melt-blending process.

Table 2
Tensile properties of the different nanocomposites at room temperature: tensile strength at yield (σ_y), strain at break (ε_b), experimental (E_{exp}) and calculated (E_{cal}) Young's modulus.

SWCNT (wt%)	WS_2 (wt%)	σ_y (MPa)	ε_b (%)	E_{exp} (GPa)	E_{cal} (GPa)	$(E_{cal}-E_{exp})/E_{exp}$ (%)
0	0	125 ± 1	12.3 ± 0.4	4.11 ± 0.07	–	–
1	0	132 ± 1	6.7 ± 0.4	4.73 ± 0.13	5.34[a]	+12.9
0	1	139 ± 2	9.3 ± 0.4	5.30 ± 0.09	4.35[a]	−17.9

SWCNT (wt%)	WS_2 (wt%)	σ_y (MPa)	ε_b (%)	E_{exp} (GPa)	Model 1	Model 2	Model 1	Model 2
0.1	0.9	143 ± 2	10.0 ± 0.5	5.58 ± 0.10	4.47	4.85	−19.8	−13.0
0.5	0.5	149 ± 3	9.1 ± 0.3	5.83 ± 0.17	4.92	5.52	−15.6	−5.3
0.9	0.1	138 ± 1	8.3 ± 0.5	5.24 ± 0.14	5.24	8.65	+0.4	+65.7
0.5[b]	0.5[b]	136 ± 2	8.2 ± 0.3	5.06 ± 0.12	4.92	5.52	−1.6	+10.4
0.9[b]	0.1[b]	133 ± 3	7.4 ± 0.5	4.80 ± 0.11	5.24	8.65	+9.1	+80.2

Models 1 and 2 refer, respectively to the modified rule of mixtures and the combination of this approach with the Halpin–Tsai equation (see explanation in the text).
[a] Values calculated through the Krenchel's rule of mixtures.
[b] Nanocomposites obtained by a two-step melt-blending process.

IF-WS_2 decreases it by about 12%. This indicates the more effective restriction ability on chain motion caused by the addition of the nanoparticles in comparison with the nanotubes, as already indicated by the T_g data; the different behaviour should be owed to the improved nanoparticle dispersion within the matrix, since the SWCNTs have strong tendency to form agglomerates due to their large surface area and strong van der Waals forces, as revealed by previous works [18,19]. Focusing on the hybrids, it can be observed that all of them show a decrease in the height of tan δ_{max} in comparison to the pure matrix. This diminution is systematically stronger for nanocomposites prepared in a single stage, in agreement with their improved SWCNT dispersion. The largest decrease (~25%) is found for the composite reinforced with the same amount of both nanofillers, which is consistent with the fact that this sample shows the highest E' and T_g.

On the other hand, the width of tan δ peak can be related with the strength of the filler–matrix interactions. The nanofillers perturb the relaxation of neighbour polymer chains, which would behave differently from those located in a further region, leading to a wider maximum. Moreover, the broadening is also probably related to the heterogeneous nature of the hybrids. Similar effect has been previously reported for different PEEK based nanocomposites [17,23], attributed to a more inhomogeneous amorphous phase in the composites in relation to the pure matrix. The data for width at half maximum value (β) are displayed in Table 1. β of pure PEEK is approximately 19 °C and increases by about 6 and 3 °C with the incorporation of 1.0 wt% SWCNTs or IF-WS_2, respectively. In the case of multiphase composites prepared in a single stage, the increment in β is around 5 and 11 °C for x/y = 0.9/0.1 and 0.5/0.5, respectively. This is consistent with the changes observed in the absorption peaks of the IR spectra of the nanocomposites in comparison to the neat polymer (see Supplementary Information), which revealed stronger SWCNT–matrix interfacial interactions for the sample incorporating the same amount of both nanofillers. Nevertheless, for similar hybrids processed in two steps, the broadening of the peak is less pronounced, suggesting weaker SWCNT–matrix interfacial adhesion. Overall, the tests performed confirm that the concurrent incorporation of both nanofillers is a very effective way to enhance the dynamic mechanical properties of PEEK.

3.2. Tensile behaviour: experimental and theoretical predictions

Typical room temperature stress–strain curves of the different nanocomposites are depicted in Fig. 2. The average in-plane Young's modulus (E), strength at yield (σ_y) and strain at break (ε_b) obtained from the tensile tests of the various samples are summarized in Table 2. As can be observed, binary composites reinforced with 1.0 wt% SWCNTs or IF-WS_2 exhibit about 15 and 28% higher modulus than the pure matrix, respectively. With respect to the hybrids prepared by concurrent addition of both nanofillers, the enhancements are in the range 27–42% (being maximum for the composite with x/y = 0.5/0.5), whilst those manufactured in two stages show increments between 17 and 24%. It is important to note that these increases are in very good agreement with those derived from DMA experiments, being the differences between the Young's and storage modulus at 25 °C lower than 8%, which confirms the validity of the results. Regarding the strength at yield, the trends observed are qualitatively similar to those described for the modulus, albeit the improvements are significantly smaller, indicating that these fillers are less effective in enhancing the strength than the stiffness of the matrix, as suggested by previous works [20,23]; the largest σ_y increment (~20%) occurs again in the sample prepared in a single step with x/y = 0.5/0.5. Focusing on the strain at break of the matrix, a strong decrease is found upon addition of 1.0 wt% SWCNTs, almost double than the attained by the incorporation of the same amount of nanoparticles; this should be related to the quasi-spherical shape of the IF-WS_2 that leads to more free volume space between them, enabling the polymer chains to deform in a more mobile manner. The hybrids prepared by a single-stage process exhibit higher tensile elongation than the two-step counterparts, suggesting higher degree of nanotube debundling and disentanglement in those composites; the largest differences are found for samples with the same amount of both nanofillers, which

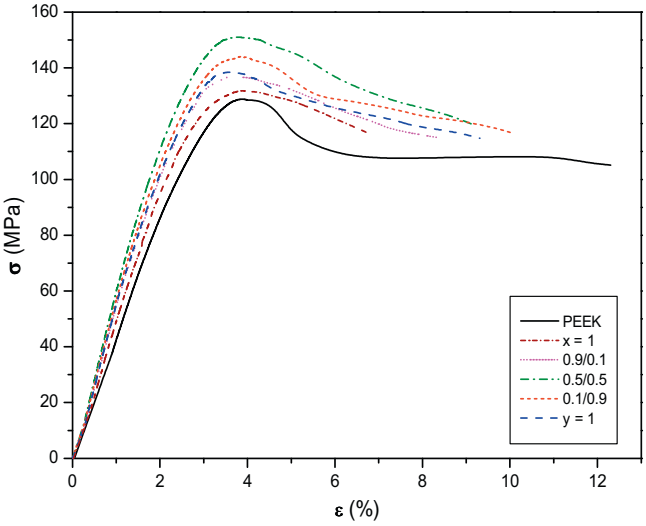

Fig. 2. Representative stress–strain curves at room temperature for the different PEEK based nanocomposites.

present about 25 and 34% lower ε_b as compared to that of the pure polymer. It is conceivable that, with further improvement of the nanofiller/matrix interfacial adhesion, via surface modifications, the mechanical properties can be further upgraded without the sacrifice of tensile ductility.

To predict the mechanical properties of filler reinforced composites, different models such as Halpin–Tsai equations, Kerner's expression or the modified rule of mixtures can be applied. The Halpin–Tsai equations [24] are a set of empirical relationships that enable to express the property of a composite material in terms of the properties of the matrix and the reinforcing elements considering their proportions and geometry. The expression that yields the tensile modulus of a nanocomposite can be expressed as:

$$E_c = E_m \frac{1 + 2sqV_f}{1 - qV_f} \quad (1)$$

where $q = (E_r - 1)/(E_r + 2s)$ and $E_r = E_f/E_m$, being s the aspect ratio of the reinforcement, E_c, E_f and E_m the tensile modulus of the composite, filler and matrix, respectively, and V_f the filler volume fraction. Taking E_f as 640 GPa [25], E_c of the composite including 1.0 wt% SWCNTs was predicted to be 9.16 GPa. Similar result (9.61 GPa) was obtained from the Kerner's equation, generalized by Lewis and Nielsen [26]. Both approximations provide values that deviate strongly from the experimental data. A more accurate prediction was obtained by the Krenchel's rule of mixtures for discontinuous reinforcement [27], which can be written as:

$$E_c = (\eta E_f - E_m)V_f + E_m \quad (2)$$

where the strengthening efficiency coefficient η is assumed to be 1/5 for randomly oriented fillers. According to Eq. (2), E_c of the binary PEEK/SWCNT composite was 5.34 GPa, about 13% higher than the experimental value. The fact that all these models overestimate the composite modulus is presumably due to the waviness of the SWCNTs, since the predictions are based on the assumption of straight nanotubes. Previous papers [28–30] have demonstrated that even slight nanotube curvature significantly reduces the efficiency of the reinforcement effect. Moreover, due to their high specific surface area and intrinsic van der Waals forces, SWCNTs remain gathered in bundles, and shear slippage within the bundle may occur [31], thereby limiting stress transfer. In addition, their large aspect ratio induces very high viscosity in the melt, which in turn would affect their uniform dispersion; even modest nanotube agglomeration reduces the filler modulus (a parameter in the models) in relation to that of isolated tubes. All these factors could explain that the experimental values are systematically lower than the predictions. On the other hand, considering the modulus of the bulk IF-WS_2 (~150 GPa) [32], the theoretical values for the composite with 1.0 wt% IF-WS_2 obtained by the Eqs. (1) and (2) were 4.13 and 4.35 GPa, respectively. In this case, both models underestimate the experimental data, probably due to the homogeneous nanoparticle dispersion caused by the decrease in the viscosity of the matrix. Nevertheless, the rule of mixtures provides again a more accurate estimation.

The Young's modulus of multiphase composites can be evaluated by a combination of the aforementioned models. Firstly, E_c of binary carbon nanotube-reinforced composites can be calculated through the Halpin–Tsai equation. Then, the polymer/SWCNT nanocomposite can be regarded as a new matrix to compute the modulus of the three-phase system by the rule of mixtures. The estimated values for the different hybrids and the deviations from the measured data are collected in Table 2 (model 2). On the other hand, E_c of the three-phase composite can be directly determined by the rule of mixtures, which can be written as:

$$E_c = \sum_i E_i V_i \quad (3)$$

where the subscript i refers to the three components. The moduli obtained by Eq. (3) are also included in Table 2 (model 1). For composites prepared in two stages, the values calculated by both models are higher or similar than the experimental data. In contrast, for those manufactured in a single step, the predictions are above the measured data for $x/y = 0.9/0.1$, whilst for the other weight fractions are below. As mentioned previously, the addition of the nanoparticles in a second step hardly modifies the state of dispersion of the SWCNTs; consequently, these show a small degree of agglomeration, hence are not able to express their full capability for stiffness enhancement. However, when both nanofillers are incorporated simultaneously and the nanoparticle concentration is high enough to reduce significantly the viscosity of the matrix [20], the SWCNT dispersion greatly improves, leading to a very effective reinforcing effect. Thus, the experimental values of composites with $x/y = 0.5/0.5$ and 0.1/0.9 are higher than the theoretical calculations. Both approximations predict the modulus reasonably well (deviations < 20%), except the model 2 when the nanoparticle concentration is extremely low (0.1 wt%); in this case, the nanotubes are probably gathered in large entangled bundles, whilst the models assume individual and straight fillers. It is important to note that the models predict a maximum reinforcing effect for the hybrids with $x/y = 0.9/0.1$, whilst the experimental data show the larger improvements at $x/y = 0.5/0.5$; this discrepancy can be explained taking into account that the models do not consider synergistic effects due to the presence of the two types of nanofillers.

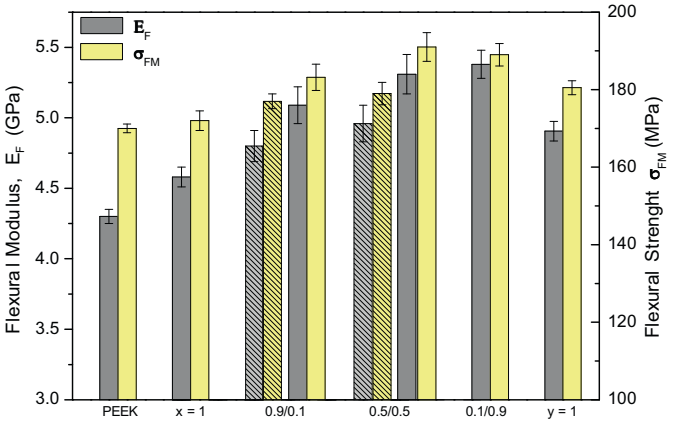

Fig. 3. Effect of SWCNTs and IF-WS_2 nanoparticles on the flexural modulus (E_F) and flexural strength (σ_{FM}) of PEEK at ambient temperature. The dashed bars correspond to samples prepared by a two-step melt-blending process.

3.3. Flexural properties

The results of flexural tests are shown in Fig. 3. The flexural modulus (E_F) of pure PEEK (~4.3 GPa) experiences about 14% enhancement with the addition of 1.0 wt% IF-WS_2, whilst improves only slightly (~6%) by the incorporation of the same amount of SWCNTs. These differences should be owed to a certain degree of nanotube clustering, as indicated previously. With regard to hybrids prepared in a single stage, the increments in E_F are in the range 20–25%, whilst for those manufactured in two steps the improvements are between 10 and 15%. On the other hand, the flexural strength (σ_{FM}) of the composite reinforced solely with SWCNTs is only marginally higher than that of PEEK (170 MPa), whereas it increases moderately (~7%) for the sample incorporating 1.0 wt%

Table 3
Room temperature average values of Charpy notched impact strength (G) for the different PEEK based nanocomposites.

SWCNT (wt%)	WS_2 (wt%)	$F(N)$	G (kJ m^{-2})
0	0	590 ± 20	5.92 ± 0.41
1	0	450 ± 30	3.53 ± 0.22
0	1	710 ± 40	5.28 ± 0.15
0.1	0.9	575 ± 40	5.70 ± 0.28
0.5	0.5	520 ± 60	5.51 ± 0.39
0.9	0.1	480 ± 50	4.92 ± 0.33
0.5[a]	0.5[a]	630 ± 10	4.45 ± 0.27
0.9[a]	0.1[a]	660 ± 30	4.04 ± 0.25

[a] Nanocomposites obtained by a two-step melt-blending process.

nanoparticles. In the case of nanocomposites manufactured by simultaneous inclusion of both fillers, σ_{FM} rises between 8 and 12%, whilst for the other hybrids increases very modestly. The improvements attained in the flexural properties are lower than those achieved in the Young's modulus and tensile strength. Taking into account that the nanofillers are randomly oriented in the three-dimensions, the nanocomposites are expected to have isotropic behaviour. Thus, the discrepancy in the reinforcing efficiency should be related to the different deformation modes of the two tests. Moreover, the larger increase in the tensile modulus could be explained considering that the tensile properties are mainly fiber-dominated, whilst the flexural properties are principally matrix-dominated [25].

3.4. Impact strength and fractography

The results obtained from room temperature Charpy impact strength measurements are collected in Table 3. The impact strength (G) of neat PEEK drops significantly by the incorporation of 1.0 wt% SWCNTs, whereas decreases only slightly upon addition of the same amount of nanoparticles. This is consistent with the reduction of the area under the stress–strain curves (Fig. 2), which is considerably more drastic for the composites reinforced solely with nanotubes. Moreover, the nanoparticles exhibit a more homogeneous dispersion within the matrix and possess quasi-spherical shape, leading to less hindrance when contacting with the polymer chains, combined with lower stress concentration at the particle/matrix interface. All these effects result in a smaller decrease of the matrix toughness.

Regarding the hybrid nanocomposites manufactured in a single stage, the impact behaviour depends strongly on the nanoparticle content. Thus, at very low IF-WS_2 concentration (x/y = 0.9/0.1), G falls by about 17% as compared to that of neat PEEK, whereas at higher nanoparticle loadings the toughness remains merely unaffected (differences < 7%). In contrast, the hybrids prepared in two stages exhibit considerably lower G than the pure matrix irrespective of their composition. These results are again related to the degree of dispersion of the nanofillers, as revealed from SEM micrographs of impact fractured specimens (Fig. 4). When similar amounts of both nanofillers are incorporated simultaneously into the matrix, the SWCNTs are randomly and well dispersed (Fig. 4a), with an average bundle diameter of ~40 nm. Some SWCNTs are found to protrude out of the matrix, suggesting that CNT pull-out instead of CNT breaking is the result of the impact fracture. Moreover, a SWCNT bridging matrix-rich regions can be observed in the micrograph, indicating that the CNTs provide reinforcement for the matrix. Therefore, the increase in fracture resistance seems to be the result of energy-dissipating mechanisms based on CNT bridging and pull-out. However, when the SWCNTs are integrated in a first step, their diameter is considerably larger (~65 nm), and small areas with CNT agglomerates can be observed (Fig. 4b); these aggregates create regions with poorer filler-matrix adhesion that require

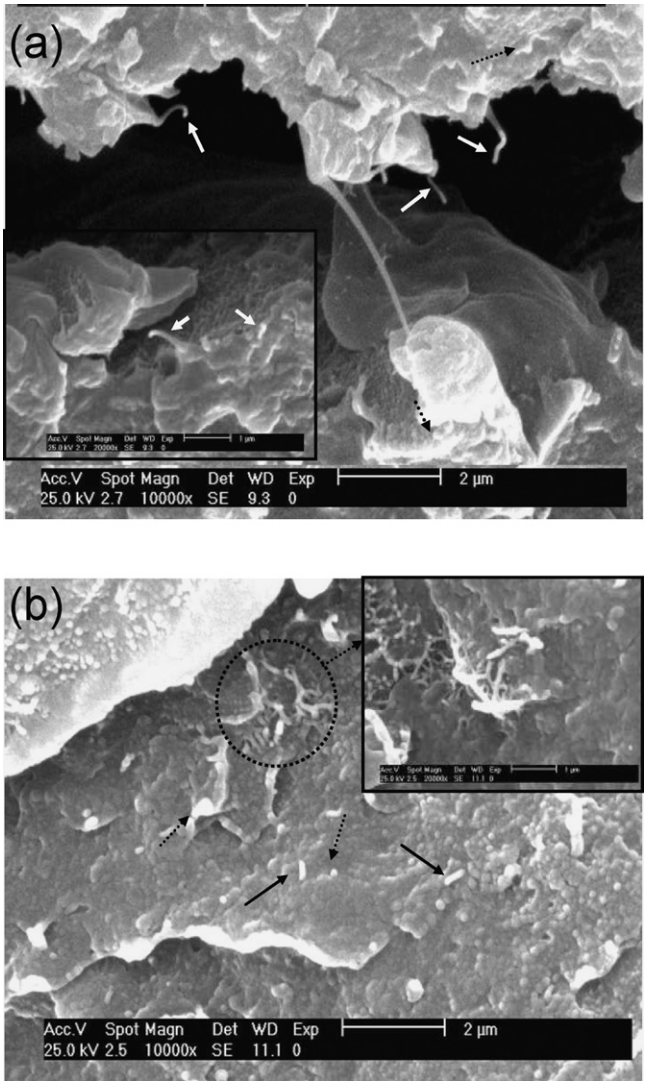

Fig. 4. Typical SEM micrographs from impact fractured surfaces of PEEK/SWCNT/IF-WS_2 (x/y = 0.5/0.5) hybrid nanocomposites prepared in a one-step process (a) and in two stages (b). The white arrows in (a) show SWCNTs pulled-out of the matrix. The black dashed and solid arrows in (b) point out nanoparticles and SWCNTs, respectively, randomly distributed through the PEEK matrix.

less energy for crack propagation, leading to premature failure. Moreover, these small agglomerates nucleate most of the cracks, increasing the brittleness of the material under high strain rates. In the case of composites including very low amount of nanoparticles, the viscosity of the matrix is very high regardless of the preparation method, hence it is very difficult to attain a perfectly homogenous SWCNT dispersion; consequently, composites with x/y = 0.9/0.1 prepared by any of the two procedures exhibit lower toughness than the neat polymer.

3.5. Temperature dependence of the electrical conductivity

The electrical conductivity (σ) is one of the most important properties of CNT-reinforced nanocomposites for potential practical applications, and depends strongly on the composition, state of dispersion of the nanofillers, manufacturing process as well as testing conditions. To analyze the influence of these parameters on the conductivity of PEEK based composites, measurements as a function of temperature were carried out (Fig. 5). It is important to note that the IF-WS_2 nanoparticles are semiconducting materials [33], and do not improve the electrical properties of the matrix;

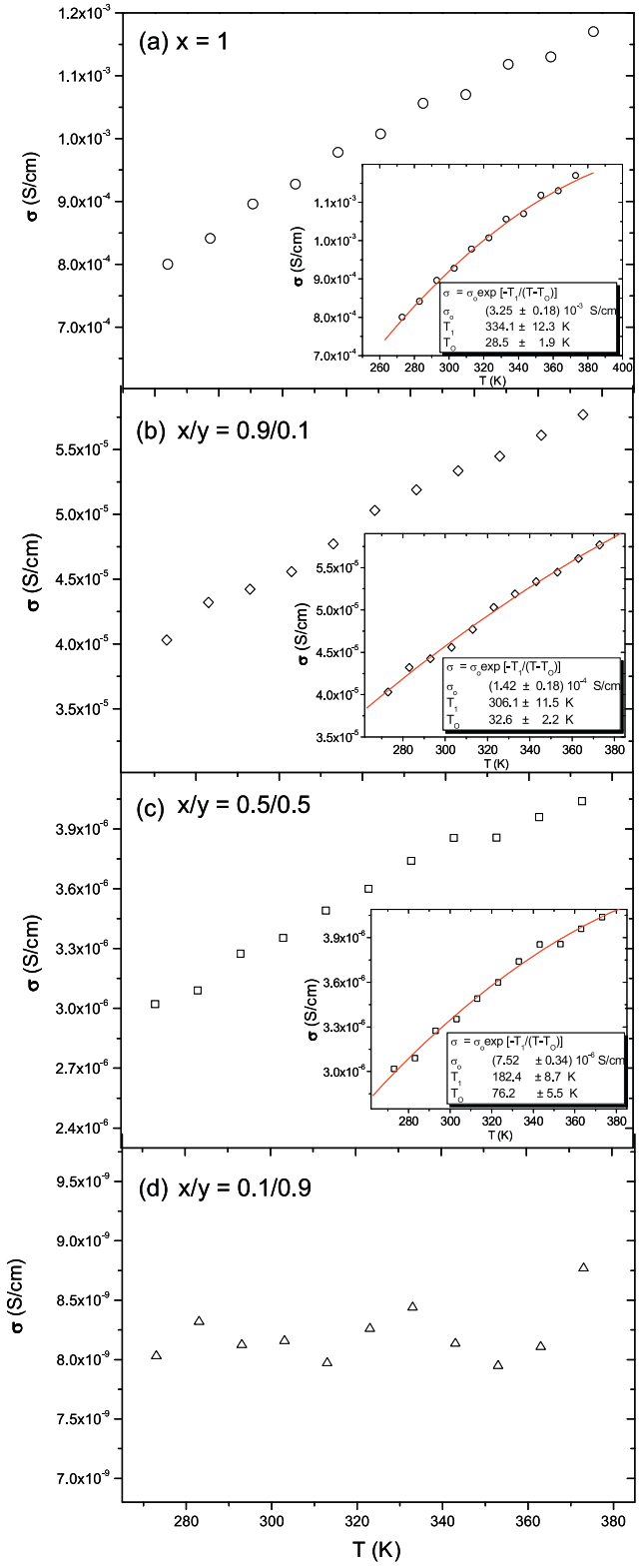

Fig. 5. Temperature dependence of the electrical conductivity of PEEK/SWCNT nanocomposite ($x = 1$) and PEEK/SWCNT/IF-WS_2 hybrid composites with different nanofiller contents. Note that PEEK and PEEK/IF-WS_2 ($y = 1$) are insulating materials ($\sigma \sim 10^{-13}$ S cm^{-1}), hence are not included in the plot.

therefore, both neat PEEK and PEEK/IF-WS_2 ($y = 1$) are electrically insulating ($\sigma \sim 10^{-13}$ S cm^{-1}) [19]. The binary composite reinforced with 1.0 wt% SWCNTs (Fig. 5a) exhibits an average σ enhancement of ten orders of magnitude in comparison with the pure matrix. This is consistent with the results obtained from previous works on PEEK/SWCNT composites [19,23], which revealed that the percolation threshold (concentration at which takes place the formation of a three-dimensional conductive network of fillers) lies slightly below 0.1 wt%. All the hybrids display lower σ than the binary sample ($x = 1$), and the composite conductivity rises with increasing SWCNT loading, showing a percolation threshold between 0.1 and 0.5 wt% nanotube content. Thus, the hybrid prepared in a single stage with $x/y = 0.1/0.9$ remains insulating ($\sigma < 10^{-8}$ S cm^{-1}) within the entire measured range, and its conductivity hardly changes with temperature (Fig. 5d). In contrast, σ of the nanocomposites with $x/y = 0.5/0.5$ and $0.9/0.1$ ($\sim 3 \times 10^{-6}$ and 4×10^{-5} S cm^{-1} at 25 °C, respectively) rises as the temperature increases following a non-linear tendency (Fig. 5b and c), indicating typical semiconducting behaviour. Moreover, the change in σ diminishes as the nanotube content decreases. Analogous trends were found for samples prepared in a two-step process (data not shown), although their σ values were about one order of magnitude lower ($\sigma_{25\,^\circ C} \sim 4 \times 10^{-6}$ and 2×10^{-5} S cm^{-1} for $x/y = 0.9/0.1$ and $0.5/0.5$, respectively). The discrepancies should be again related to differences in the state of dispersion of the nanofillers; as mentioned previously, the nanotubes are more disentangled and debundled in composites manufactured in a single stage, hence possess higher aspect ratio, which results in higher conductivity values.

Different models have been proposed to explain the temperature dependence of σ, such as the 3D variable-range hopping (VRH) [34] or the thermal fluctuation-induced tunnelling (FIT) mechanism [35]. In the case of PEEK/SWCNT nanocomposites, the nanotubes are surrounded by an insulating polymer, which acts as a potential barrier to inter-tube hopping; therefore, the composite conductivity could be explained by quantum tunnelling theory in which the barrier height diminishes as the temperature rises. This behaviour can be described by the FIT model proposed by Sheng [35] as follows:

$$\sigma = \sigma_0 \exp\left(-\frac{T_1}{T - T_0}\right) \quad (4)$$

where σ_0 is the conductivity at infinite temperature, T_1 represents the energy required for an electron to cross the insulator gap between conductive clusters and is related to the activation energy, and T_0 is the temperature above which the thermal activated conduction over the barrier begins to occur [36]. As can be observed in the inset of Fig. 5a–c, the predictions of the FIT model concur greatly with the experimental data of composites manufactured in a single stage with $x \geq 0.5$ wt%; a good correlation was also observed for similar hybrid nanocomposites prepared in two stages. This corroborates that the electrical conduction in these composites is hindered by potential barriers between neighbouring nanotube bundles due to the polymer wrapping. As expected, the characteristic temperature T_0 decreases with increasing SWCNT loading, indicating that the charge-carrier generation process occurs at lower temperatures. Overall, our results demonstrate that the electrical conductivity of these hybrids can be tailored by modifying the concentration of both nanofillers, making them suitable for specific applications such as electrostatic dissipation or electrostatic painting.

4. Conclusions

The mechanical and electrical properties of high-performance PEEK based hybrid nanocomposites incorporating SWCNTs and IF-WS_2 nanoparticles have been analyzed both experimentally and theoretically. The addition of very low loadings of both nanofillers (≤1.0 wt%) led to a noticeable increase in the storage modulus, glass transition temperature, Young's modulus and tensile strength of the matrix, attributed to synergistic reinforcement effects combined with strong PEEK–SWCNT interfacial interactions.

Nevertheless, the ductility and toughness slightly decreased, albeit were well above the values of binary PEEK/SWCNT composites. A combination of the Halpin–Tsai equation or the Maxwell model with the rule of mixtures was applied to predict the Young's modulus of these nanocomposites. The hybrids with 0.1 wt% SWCNT content remained electrically insulating, whilst those incorporating higher loadings exhibited semiconducting behaviour, and the temperature dependence of their electrical conductivity followed a fluctuation-induced tunnelling model. Samples manufactured through a one-step melt-blending process displayed improved overall performance than those prepared in two stages, ascribed to an enhanced nanofiller dispersion. The tests performed confirm that the incorporation of both nanofillers in different weight fractions provides multifunctional high-performance materials for the fabrication of nanodevices or lightweight structures suitable to be used in industrial applications (i.e. aeronautic, aerospace, automobile). This approach is a simple and scalable method that could be employed for the synthesis of different multiphase thermoplastic/CNT/metal nanoparticle nanocomposites with diverse functionalities.

Acknowledgments

Dr. A. Diez would like to thank to the Spanish Ministry of Science and Innovation (MICINN) for Juan de la Cierva contract and Dr. M. Naffakh to the Consejo Superior de Investigaciones Científicas (CSIC) for postdoctoral contract.

Appendix A. Supplementary data

Supplementary data associated with this article can be found, in the online version, at doi:10.1016/j.matchemphys.2011.06.019.

References

[1] S. Iijima, T. Ichihaschi, Nature 363 (1993) 603–605.
[2] M.S. Dresselhaus, G. Dresselhaus, P.C. Eklund, Science of Fullerenes and Carbon Nanotubes, Academic Press, San Diego, 1996.
[3] X. Gong, J. Liu, S. Baskaran, R.D. Voise, J.S. Young, Chem. Mater. 12 (2000) 149–152.
[4] M.S. Shaffer, A.H. Windle, Adv. Mater. 11 (1999) 937–941.
[5] A. Star, J.F. Stoddart, D. Steuerman, A. Boukai, E.W. Wong, X. Yang, S. Chung, J.R. Heath, Angew. Chem. Int. Ed. Engl. 40 (2001) 1721–1725.
[6] M. Olek, K. Kempa, S. Jurga, M. Giersig, Langmuir 21 (2005) 3146–3152.
[7] K.R. Reddy, B.C. Sin, K.S. Ryu, J.-C. Kim, H. Chung, Y. Lee, Synth. Met. 159 (2009) 595–603.
[8] J. Lin, C. He, Y. Zhao, S. Zhang, Sens. Actuators B 137 (2009) 768–773.
[9] R. Tenne, L. Margulis, M. Genut, G.R. Hodes, Nature 360 (1992) 444–445.
[10] L. Rapoport, N. Fleischer, R. Tenne, J. Mater. Chem. 15 (2005) 1782–1788.
[11] L. Rapoport, O. Nepomnyashchy, R. Popovitz-Biro, Y. Volovik, B. Ittah, R. Tenne, Adv. Eng. Mater. 6 (2004) 44–48.
[12] M. Naffakh, Z. Martín, N. Fanegas, C. Marco, M.A. Gómez, I. Jiménez, J. Polym. Sci. Part B: Polym. Phys. 45 (2007) 2309–2321.
[13] M. Naffakh, C. Marco, M.A. Gómez, I. Jiménez, J. Phys. Chem. B 112 (2008) 14819–14828.
[14] O.B. Searle, R.H. Pfeiffer, Polym. Eng. Sci. 25 (1985) 474–476.
[15] D.P. Jones, D.C. Leach, D.R. Moore, Polymer 26 (1985) 1385–1393.
[16] J. Sandler, A.H. Windle, P. Werner, V. Altstadt, M.S.P. Shaffer, J. Mater. Sci. 38 (2003) 2135–2141.
[17] J. Sandler, P. Werner, M.S.P. Shaffer, V. Demchuck, V. Altstadt, A.H. Windle, Compos. Part A 33 (2002) 1033–1039.
[18] A.M. Diez-Pascual, M. Naffakh, M.A. Gómez, C. Marco, G. Ellis, M.T. Martínez, A. Ansón, J.M. González-Domínguez, Y. Martínez-Rubi, B. Simard, Carbon 47 (2009) 3079–3090.
[19] A.M. Diez-Pascual, M. Naffakh, M.A. Gómez, C. Marco, G. Ellis, M.T. Martínez, A. Ansón, J.M. González-Domínguez, Y. Martínez-Rubi, B. Simard, B. Asrhafi, Nanotechnology 20 (2009) 315707–315720.
[20] M. Naffakh, A.M. Diez-Pascual, C. Marco, M.A. Gómez, I. Jiménez, J. Phys. Chem. B 114 (2010) 11444–11453.
[21] M. Naffakh, A.M. Diez-Pascual, M.A. Gómez, J. Mater. Chem. 21 (2011) 7425–7433.
[22] J.P. Lu, Phys. Rev. Lett. 79 (1997) 1297–1300.
[23] A.M. Diez-Pascual, M. Naffakh, M.A. Gómez, M.T. Martínez, A. Ansón, J.M. González-Domínguez, Y. Martínez-Rubi, B. Simard, Carbon 48 (2010) 3500–3511.
[24] J.C. Halpin, L.C. Kardos, Polym. Eng. Sci. 16 (1976) 344–352.
[25] M. Kim, Y.-B. Park, O.I. Okoli, C. Zhang, Compos. Sci. Technol. 69 (2009) 335–342.
[26] T. Lewis, L. Nielsen, J. Appl. Polym. Sci. 14 (1970) 1449–1471.
[27] H. Krenchel, Fibre Reinforcement, Akademisk Forlag, Copenhagen, 1964.
[28] F.T. Fisher, R.D. Bradshaw, L.C. Brinson, Compos. Sci. Technol. 63 (2003) 1689–1703.
[29] R.D. Bradshaw, F.T. Fisher, L.C. Brinson, Compos. Sci. Technol. 63 (2003) 1705–1722.
[30] V. Anumandla, R.F. Gibson, Compos. Part A 37 (2006) 2178–2185.
[31] S. Xie, W. Li, Z. Pan, B. Chang, L. Sun, J. Phys. Chem. Solids 61 (2000) 1153–1158.
[32] O. Tevet, O. Goldbart, S.R. Cohen, R. Rosentsveig, R. Popovitz-Biro, H.D. Wagner, R. Tenne, Nanotechnology 21 (2010) 365705 (6pp), doi:10.1088/0957-4484/21/36/365705.
[33] F. Kopnov, A. Yoffe, G. Leitus, R. Tenne, Phys. Status Solidi B 243 (2006) 1229–1240.
[34] N.F. Mott, E.A. Davis, Electronic Processes in Non-Crystalline Materials, second ed., Clarendon Press, Oxford, 1979.
[35] P. Sheng, Phys. Rev. B 21 (1980) 2180–2195.
[36] E. Kymakis, G.A.J. Amaratunga, J. Appl. Phys. 99 (2006) 84302–84308.